Self-Consistent Field Calculations of Tethered Chains in the Presence of Mobile Homopolymer: Comparison with Experiment

Christopher M. Wijmans*

Physical Chemistry 1, Center for Chemistry and Chemical Engineering, University of Lund, P.O. Box 124 , S-221 00, Lund, Sweden

Bradford J. Factor†

Polymers Division, Material Science and Engineering Laboratory, National Institute of Standards and Technology, Gaithersburg, Maryland 20899

Received September 18, 1995; Revised Manuscript Received February 21, 1996⊗

ABSTRACT: Concentration profiles of tethered polymer chains in the presence of mobile homopolymer under good solvent conditions have been calculated using self-consistent field (SCF) methods which incorporated the experimental conditions of a recent neutron reflectivity study by Lee et al. [*J. Chem. Soc., Faraday Discuss.* **1994**, *98*, 139]. While there is good qualitative agreement between the experimental results and the SCF calculations, the calculations predict a larger decrease in the tethered layer heights than is observed in the experiments. Furthermore, with increasing mobile polymer molecular weight, the calculations predict concentration profile shapes which become more *steplike.* The feasibility of discerning this effect using either neutron reflectivity or small angle neutron scattering is discussed.

Introduction

Polymer chains which are attached at one end to a surface, so called *tethered chains*, have received much attention in experimental and theoretical studies in recent years.[1,2] The field has been motivated, in part, by the prospects for technological applications of dense layers of tethered polymers, for example, in lubrication and colloidal stabilization. In the present work, we are concerned with how the presence of mobile homopolymers affects the structure of the tethered polymer layer under good solvent conditions.

Theoretical models by de Gennes,[3] Gast and Leibler,[4] Zhulina et al.,[5] Wijmans et al.,[6] and van Zanten[7] predict that the presence of mobile polymers alters the balance of elastic forces and excluded volume interactions which exists in tethered polymer chains. At a sufficiently large concentration under good solvent conditions, the mobile chains penetrate into the tethered polymer layer. This causes the excluded volume interactions among the tethered chains to be screened, resulting in a decrease of the tethered layer thickness. Similar effects occur in polymer melts where sufficiently short homopolymer chains penetrate into the tethered layer, while longer chains are excluded.[8,9]

Recently, Lee et al.[10] have observed a reduction in the tethered layer thickness upon the addition of mobile homopolymer under good solvent conditions using neutron reflectivity. As the grafting density and degree of polymer stretching observed in this experiment are much smaller than that assumed in the calculations,[3−7] it is not possible to make a quantitative comparison between experiment and theory. To enable an appropriate quantitative comparison, we have performed SCF calculations which correspond to the experimental conditions of Lee et al.[10] The results of the SCF calculations are the subject of this article.

* To whom correspondence should be addressed.

† Present address: Intel Corp., CH5-137, 5000 W. Chandler Blvd., Chandler, AZ 85226.

⊗ Abstract published in *Advance ACS Abstracts,* May 1, 1996.

Theoretical Calculations

A lattice-based self-consistent theory (SCF) is used to model the experimental system. A detailed description of this approach can be found in the literature.[11−13] The basic idea is that all possible lattice conformations of the grafted and free chains are generated on a lattice, which is a simple cubic lattice in our case. Each conformation is weighted by an appropriate Boltzmann factor in order to find the equilibrium distribution of free and grafted polymer. The grafted chains are assumed to be attached to an infinite, hard surface. The solution is divided into parallel layers, numbered $z = 1, 2, 3, ...$, starting with the layer adjacent to the surface. The lattice spacing l is taken to be the polymer segment diameter. Within each layer, a mean-field approximation is applied so that gradients occur only perpendicular to the surface.

In the SCF approach, the polymer chains are normally treated as freely jointed chains, consisting of N_g segments numbered $s = 1, 2, 3, ..., N_g$. For the present calculations, however, the chains are modeled with a limited bond flexibility. A motivation for this slightly more elaborate approach will be given below. First, we briefly present the method, which is analogous to previous models in the literature.[12−14]

In the *classical* implementation of the SCF theory, all possible chain conformations are treated identically. Conformations where direct back-folding occurs are excluded; that is, a segment s may not occupy the same lattice site as segment $s - 2$. Furthermore, we introduce an energy difference U^b between the two conformations in which two consecutive bonds form either an angle of 180° or 90°. Both the exclusion of direct back-folding and the introduction of this bending energy U^b increase the stiffness of the polymer chain. In the freely jointed chain model, each segment is a Kuhn segment. Now, the ratio p between the Kuhn length and the bond length l (i.e., the lattice spacing) is

$$p = 1 + {}^1/_2 \exp(\beta U^b) \qquad (1)$$

where $\beta = (k_B T)^{-1}$. A more detailed description of this model for grafted chains with a limited bond flexibility is given in ref 13. In our case, the only difference with ref 13 is that the system also contains free polymer which is chemically identical to the grafted polymer but does not necessarily have the same degree of polymerization. The free polymer is also modeled using the limited bond flexibility description. The extension of the SCF theory to include the equilibrium with a solution of polymer chains with chain length N_f and volume fraction Φ is straightforward (see ref 12, for example).

S0024-9297(95)01402-1 CCC: $12.00

Parameters. In order to compare the experimental data with the lattice theory, it is necessary to develop a scaling procedure to determine the chain length and bending energy in the lattice model. We base this scaling procedure on the equivalence of the contour length, radius of gyration, and volume of a real polymer and a polymer chain in the lattice model. The equivalence of the contour length gives

$$Nl = \frac{M}{M_s} l_b \tag{2}$$

where N is the degree of polymerization on the lattice, l is the lattice spacing, M is the polymer molecular weight, M_s is the monomer molecular weight, and l_b is the bond length between two monomers. Similarly, the equivalence of the volume yields

$$Nl^3 = M/\rho N_{AV} \tag{3}$$

where ρ is the density of the polymer, and N_{AV} is the Avogadro number. Finally, the equivalence of the radius of gyration gives the following equation:

$$^1/_6\, pl^2\, N = a^2\, M \tag{4}$$

where p is determined by the value of U^b according to eq 1 and a is defined as $R_g/M^{1/2}$.

For the grafted d-PS chains $M = 1.7 \times 10^5$, $M_s = 112.5$, $l_b = 0.25$ nm, $\rho = 1.13 \times 10^3$ kg/m^3, and $a = 0.3$ nm. This leads to the following values for the lattice model parameters: $N = 464$, $l = 0.815$ nm, $p = 2.98$ (or $U^b = 1.38 k_B T$). The grafting density σ in the lattice model is proportional to the experimentally determined grafting density σ_e (nm^{-2}): $\sigma = (0.815)^2 \sigma_e$. The homopolymer concentration, c, is given in units of g/cm^3; the corresponding volume fraction, Φ, is given by $0.095c$ for polystyrene (h-PS). Thus, the only undetermined parameter that remains is χ. Unfortunately, no accurate measurement has been made of this parameter for PS in ethyl benzoate (EB). The close agreement between the radius of gyration of PS in toluene and in EB suggests that $\chi \approx 0.4$, which is the measured value for toluene.[15] But, as we do not know how accurate this value is, we have also varied the value of χ in the computations.

We would like to point out that there are two cases of tethered chains in the literature:[1] (i) chemically grafted polymers where grafting points remain fixed and (ii) adsorbing polymers where the adsorption is due to either an end group or an adsorbing block of a diblock copolymer. In the latter case, which corresponds to the experiments of Lee et al.,[10] the grafting points have freedom to move. In our calculations, we have not distinguished between these two cases. For the limit of small grafting densities, however, there may be differences. For the case of grafted chains where the neighboring tethered chains do not overlap, the distribution of grafting points may be inhomogeneous, particularly if grafting occurred in a poor solvent.[16] By contrast, the copolymer layers considered in our paper are free to move along the surface, and, on average, the lateral distribution is expected to be homogeneous.

Results

In the experiments by Lee et al.,[10] the tethered polymer layer consists of poly(dimethylsiloxane)-*b*-*d*-polystyrene diblock copolymers, denoted PDMS-PS, which have been spread on the surface of an ethyl benzoate solution containing polystyrene homopolymer. Tethered layers consisting of 21K PDMS and 169K *deuterated* PS blocks, denoted 20K−170K, were spread on a variety of solutions containing different *nondeuterated* PS homopolymer molecular weights and concentrations. The tethered block is deuterated, providing contrast in scattering length density for the neutron reflectivity (NR) experiments. The reflectivity data were fitted using parabolic tethered polymer concentration profiles. The profiles usually exhibit a depletion layer at the air surface and an exponential decay at the solution interface. Further details about the PDMS-PS system examined in pure solvent and the corresponding concentration profiles as well as details of the experimental procedure are given elsewhere.[17] It should also be noted that, aside from acting as a junction point at the solution surface, the PDMS block is assumed not to affect the concentration profile of either the tethered or mobile polymers.

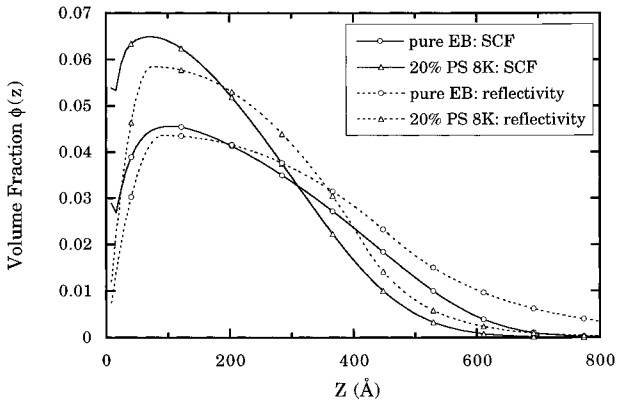

Figure 1. Comparison between concentration profiles for 20K−170K PDMS-PS in $c = 20\%$ 8K PS homopolymer solvent (△) ($\sigma = 8.0 \times 10^{-5}$ Å^{-2}) and the pure solvent (○; ($\sigma = 7.1 \times 10^{-5}$ Å^{-2}) calculated by the SCF method using $\chi = 0.25$ (—). Parabolic profiles (- -) which have been fitted to the reflectivity data are also shown.

Several SCF calculations were performed using the molecular weights and concentrations of the homopolymer solutions and the grafting densities σ as determined from NR. In Figure 1, a comparison is made between the SCF calculations and the fitted parabolic profiles for a tethered polymer layer with a grafting density of $\sigma = 8.0 \times 10^{-5}$ Å^{-2} in a $c = 20\%$ 8K PS homopolymer solution, as well as the case of $\sigma = 7.1 \times 10^{-5}$ Å^{-2} where no homopolymer is present. An interaction parameter of $\chi = 0.25$ was used in the SCF calculations. The corresponding calculated reflectivity profiles are compared to the reflectivity data in Figure 2. It is clear in Figure 1 that there is a significant decrease in the layer height due to the presence of the homopolymer. Furthermore, there are differences in the shape between the SCF and parabolic profiles; in particular, the SCF profiles have a smaller depletion layer and then a decay which is between linear and parabolic. Finally, we note that there is reasonable agreement between the reflectivities calculated from the SCF profiles and the actual data.

To compare the dimensions of the SCF model profile with that fitted from reflectivity, it was most convenient to use the mean layer height (first moment) given by the expression

$$h_{av} = \frac{\int_0^\infty z\phi(z)\, dz}{\int_0^\infty \phi(z)\, dz} \tag{5}$$

where $\phi(z)$ is the volume fraction of the tethered polymer. Root mean square values were also calculated, and the results, while quantitatively larger, show the same qualitative trends. Comparisons of h_{av} vs σ values determined from SCF models with $\chi = 0.4$ and $\chi = 0.25$ and NR are given in Figures 3−5 . For the tethered layer on pure EB solvent, shown in Figure 3, the NR values for h_{av} vary from 200 to 280 Å over the measured

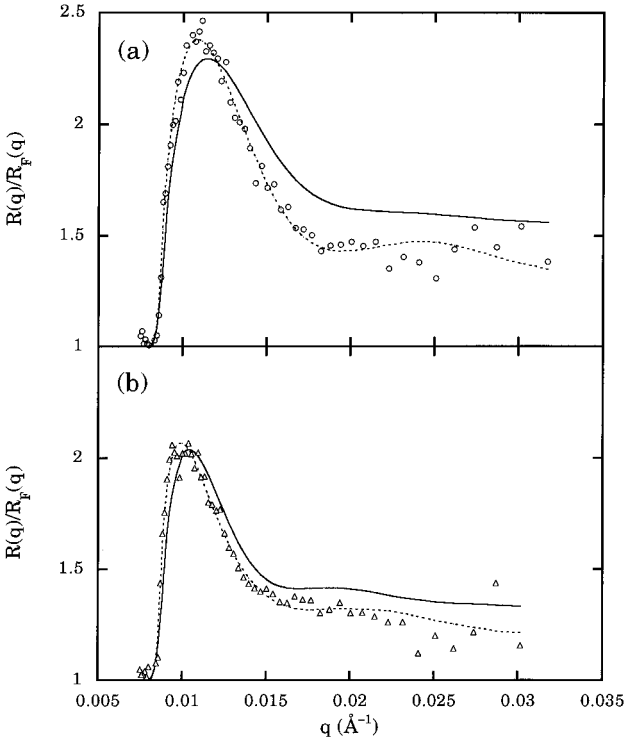

Figure 2. Neutron reflectivity data and reflectivity profiles calculated from SCF (—) and parabolic concentration profiles (- -) shown in Figure 1: (a) $c = 20\%$ 8K PS solutions; (b) pure EB solution.

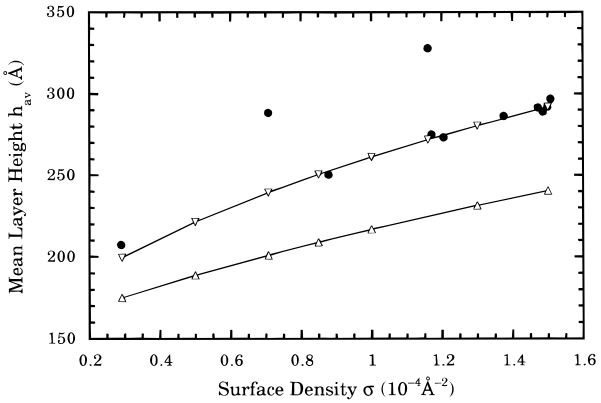

Figure 3. Mean layer height vs σ values for 20K−170K PDMS-PS in pure EB solvent computed using SCF method using $\chi = 0.4$ (△) and $\chi = 0.25$ (▽) and from parabolic fits to the reflectivity data (●). The solid lines are a guide to the eye.

range of σ. The reflectivity results agree well with the $\chi = 0.25$ SCF models, except for the two data points where h_{av} are about 50 Å larger. We believe that the reason for this discrepancy is that they were fitted using a parabolic profile which included both a depletion layer and an exponential tail, while the points which display better agreement were fitted with a purely parabolic profile with no additional features. The depletion layer and the exponential tail have the effect of systematically increasing h_{av}. The $\chi = 0.4$ models, on the other hand, are all too low, by at least 50 Å.

Results for the 10% PS 43K solution are shown in Figure 4. For a given σ value, the h_{av} values from the NR data are about 50 Å less than those for the pure EB case. The SCF results also show a large reduction in h_{av} when 10% PS 43K homopolymer is added to the EB solvent. The magnitude of the decrease depends on χ as well as σ. For $\chi = 0.25$, h_{av} has decreased by 60−80 Å, which is greater than for the NR results. For $\chi =$

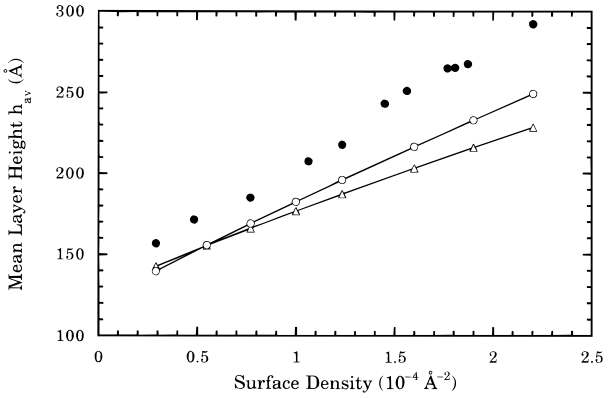

Figure 4. Mean layer height h_{av} vs σ values for 20K−170K PDMS-PS in $c = 10\%$ 43K PS solution computed using the SCF method with $\chi = 0.4$ (△) and $\chi = 0.25$ (○) and from parabolic fits to the reflectivity data (●). The solid lines are guides to the eye.

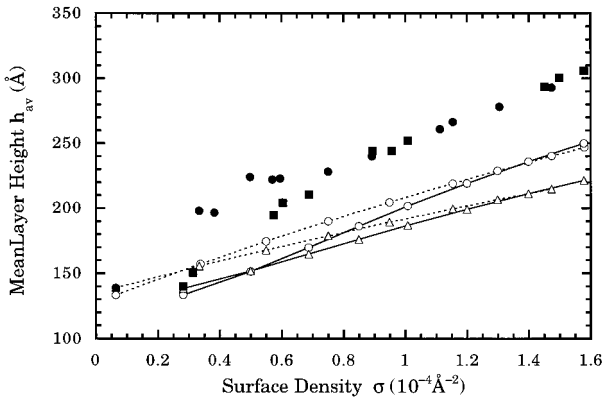

Figure 5. Mean layer height vs σ values for 20K−170K PDMS-PS in $c = 6\%$ 43K PS and 400K solutions. The results from the SCF method for the 43K PS are indicated with the dotted lines with (△) for $\chi = 0.4$ and (○) for $\chi = 0.25$, while those from the 400K PS are indicated by the solid lines with (△) for $\chi = 0.4$ and (○) for $\chi = 0.25$. The results from fits to parabolic profiles are indicated by (●) and (■) for 43K and 400K PS, respectively.

0.4, on the other hand, h_{av} decreases by 30−40 Å, which is less than for the NR results. For both $\chi = 0.25$ and $\chi = 0.4$, the magnitude of the decrease increases slightly as a function of σ. Also, the calculated profiles are nearly the same at low σ. However, as σ increases, the h_{av} values for $\chi = 0.25$ are greater than for $\chi = 0.4$.

Figure 5 compares the SCF models and NR results for $c = 6\%$ data for both 43K and 400K PS homopolymers. The NR results for the 43K and 400K cases appear to be equivalent for $\sigma > 8 \times 10^{-5}$ Å^{-2}. For $\sigma < 8 \times 10^{-5}$ Å^{-2}, the data for 43K homopolymer are 30−50 Å greater than for the 400K case. The SCF results are consistent with this observation. At low σ, the SCF models for 43K PS give somewhat larger layer heights than those for the 400K case, while, at large σ, the results merge. Next, with comparison of the layer heights where $\chi = 0.4$ and $\chi = 0.25$ for a fixed homopolymer molecular weight, the profiles are nearly the same at low σ. However, as σ increases, h_{av} for calculations using $\chi = 0.25$ are larger than those using $\chi = 0.4$. This is the same trend as for the 10% PS 43K case.

In Figure 6, a detailed comparison between the SCF models ($\chi = 0.25$) for the $c = 6\%$ 43K and 400K PS cases indicates that the tethered layer is more *steplike* at larger σ for the larger molecular weight homopolymer. There are corresponding differences in the mobile

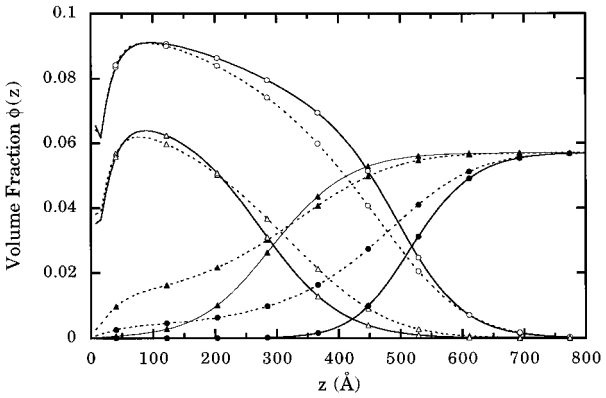

Figure 6. SCF concentration profiles ($\chi = 0.25$) corresponding to the d−PS 170K tethered polymer in contact with mobile polymer solution of $c = 6\%$ 43K (- -) at $\sigma = 7.6 \times 10^{-5}$ Å^{-2} (△) and $\sigma = 1.47 \times 10^{-4}$ (○) Å^{-2}, and for $c = 6\%$ 400K (—) at $\sigma = 6.9 \times 10^{-5}$ Å^{-2} (△) and $\sigma = 1.58 \times 10^{-4}$ Å^{-2} (○). The tethered polymer and mobile polymer profiles are shown by the open and filled symbols, respectively. At the higher grafting density, the concentration profile is more steplike for the 400K case and, correspondingly, more homopolymer is excluded from tethered layer.

polymer concentration profiles where less 400K homopolymer penetrated into the tethered layer than 43K homopolymer. The prospects for using experiments to distinguish between the two profiles are discussed in the next section.

Discussion

We have introduced a new procedure to model experimental systems of interfacial polymer layers using a lattice-based SCF theory. Previously, a simpler approach has been proposed to model such systems based on a freely jointed chain model for the polymer chains. For that case Fleer et al.[18] have suggested a similar method to match the theoretical parameters with the experimental data. Their approach is based on the equivalence of the radius of gyration and the contour length. However, this method grossly misrepresents the volume of a polymer chain. This means that, for a given σ value (which is experimentally determined), the area under the calculated volume fraction profile $\phi(z)$ will differ significantly from the experimental value. Consequently, it is not possible to use this method to make a quantitative comparison between the NR results and the SCF model.

Turning to Figures 3−5, we conclude that the SCF model qualitatively reproduces the decrease in the h_{av} due to the presence of the homopolymer. For $\chi = 0.25$, the quantitative agreement is also decent; however, the predicted layer heights are too small by about 30−50 Å when homopolymer is present. The agreement is overall less satisfying for the $\chi = 0.4$ calculations.

That $\chi = 0.25$ leads to better agreement than $\chi = 0.4$ might, in part, be due to the way in which the chains are modeled. Within the formalism of the lattice-based SCF theory, it is possible to model the stiffness of chains in different ways. Our choice to exclude direct back-folding and to introduce the bending energy parameter U^b is rather arbitrary. For example, the same value for the stiffness parameter p could also be found by not excluding direct back-folding and simultaneously increasing U^b. Another possibility would be to incorporate correlations between *next-nearest* bonds. These different alternatives lead to slightly different profiles and layer heights. However, although the effects of such alternatives have, to our knowledge, never been studied systematically, we surmise that, for a given value of p, the volume fraction profiles will not greatly depend on the exact way in which the stiffness has been incorporated. This hypothesis is supported by the good agreement that Wijmans et al.[13] found between this model for polymer brushes and calculations based on a different *freely jointed stiff rods* model and calculations based on a continuum description of stiff chains.

The differences between the SCF and NR results are certainly larger than what we expect to be the effect of the modeling method, as mentioned above, and seem to represent an inherent difference between the SCF theory and experiment. Yet, the agreement we have obtained is similar to other work in the literature. Baranowski and Whitmore[19] compared SCF and NR results for tethered polymers in the presence of solvent with mobile polymer. A value of $\chi = 0.44$ was used in the calculations. They obtained values for the root mean squared layer heights for 20K−170K which are systematically about 10% smaller than the NR results, similar in the quality to our results.

The SCF calculations are also reasonably consistent with the NR results with regard to the effects of homopolymer molecular weight. Comparing the results of 20% PS 8K and 10% PS 43K where $\sigma = 8.0 \times 10^{-5}$ Å^{-2} (cf. Figures 1 and 4), we remark that the layer height is nearly 10 Å smaller for the 10% PS 43K case for both SCF and NR results. As was pointed out by Lee et al.,[10] this is in agreement with the notion that the 8K PS *swells* the layer more than the 43K PS due to the larger entropy of the smaller chains. This effect was first described by Flory.[20]

The SCF profiles in Figure 6 lead us to question whether effects of homopolymer molecular weight can be observed within the experimental error of the NR technique. In particular, is it possible to distinguish between the concentration profiles for 43K and 400K PS mobile polymers? To answer this question, NR and SANS profiles have been calculated using the concentration profiles in Figure 6. Calculated reflectivity ratios $R(q)/R_F(q)$, where q [$=4\pi\sin(\theta/\lambda)$] is the scattering vector, are given in Figure 7 and calculated SANS profiles plotted as $I(q)q^4$ vs q and $I(q)q^2$ vs q are given in Figure 8.

The reflectivity was determined using the Parrat method.[21,22] This involves first calculating the reflection coefficients for the individual interfaces between the layers in the SCF model. To arrive at the reflectivity, which is the modulus of the overall reflection coefficient, the reflection coefficient of the bottom two interfaces is calculated using the Fresnel formula.[22] More layers are progressively included until the reflection coefficient from the top surface is obtained. The scattering length densities of the solvent and the deuterated PS polymer are $n_s = 1.434 \times 10^{-6}$ Å^{-2} and $n_p = 6.476 \times 10^{-6}$ Å^{-2}, respectively. The PDMS on the solvent surface has a scattering length density nearly equal to that of air, and, therefore, the PDMS does not have to be explicitly included in the calculation. In the models, a Gaussian resolution function with a full width at half-maximum of $\Delta q = 0.03q$ was used. In Figure 7a, we see that there are subtle differences in the reflectivities corresponding to the tethered polymer concentration profiles in Figure 6 (the larger σ values only). The reflectivity profile corresponding to the 400K PS homopolymer has stronger oscillations than the 43K PS case. This is due to

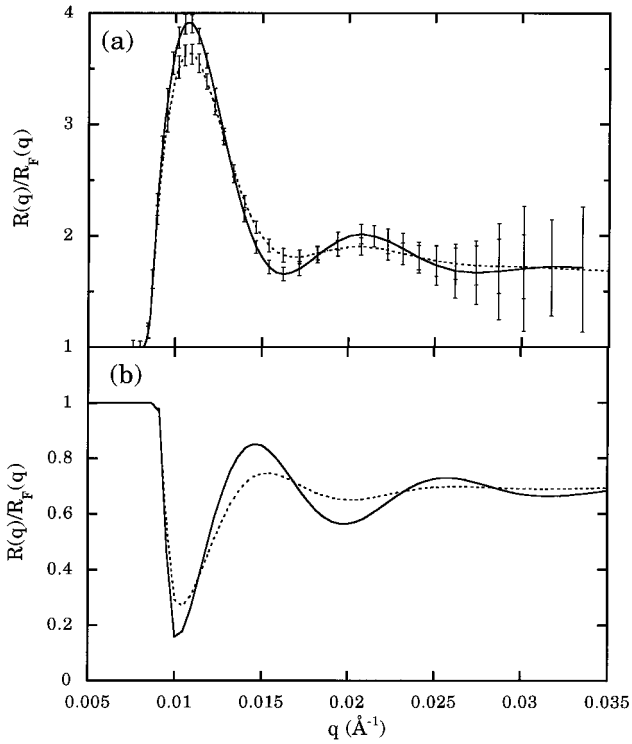

Figure 7. Calculated neutron reflectivity ratios $R(q)/R_F(q)$ corresponding to the $\sigma = 1.47 \times 10^{-4}$ Å^{-2} for 43K PS (- -) and $\sigma = 1.58 \times 10^{-4}$ Å^{-2} for 400K PS (—) concentration profiles in Figure 6. (a) d-PS tethered polymer with h-PS mobile polymer; (b) h-PS tethered polymer with d-PS mobile polymer. In both cases, the EB solvent is not deuterated.

the fact that the mobile polymer concentration for the 400K PS is more steplike.

Error bars representing the counting statistics of the DESIR reflectometer at Saclay[17] have been included in Figure 7a. With the error bars, it is possible to resolve between the 43K and 400K cases for $q < 0.02$ Å^{-1}. For $q > 0.02$ Å^{-1}, the differences between the two data sets decreased as the statistical errors increase, and therefore, the two data sets cannot be resolved in this regime. The statistical error could be made smaller by either increasing the neutron flux or the counting time. However, since the data sets are nearly equivalent at large q, the ability to resolve the two data sets would improve only marginally.

In Figure 7b, the reflectivity ratios corresponding to the case where the contrast has been inverted (i.e., only the mobile homopolymer is deuterated) is shown. The reflectivity from the 400K PS has stronger oscillations than that from the 43K PS. This is due to the fact that the mobile polymer concentration profile for the 400K PS is also more steplike. Comparing Figure 7a with Figure 7b, the differences between the 400K and 43K PS calculated reflectivies appear to be similar. While error bars have not been included in Figure 7b, the ability to resolve between the 400K and 43K data sets is expected also to be like that for Figure 7a.

Next, the small angle neutron scattering (SANS) resulting from polymer layers grafted to the surface of glass beads or porous glass has been calculated. The calculations are similar to those of Auroy et al.[23,24] and Cosgrove et al.,[25] who examined tethered layers in porous glass and silica spheres, respectively. For convenience, we have assumed a contrast match between the solvent, glass, and adsorbing polymer. The SANS intensity reduces to[23−26]

$$I(q) = \frac{2\pi S}{V} \frac{(n_p - n_s)^2}{q^2} \left| \int_0^\infty dz\, e^{iqz}\, \phi(z) \right|^2 \qquad (6)$$

where S/V is the surface to volume ratio. The predicted scattering corresponding to the tethered polymer concentration profiles of Figure 6 are shown in Figure 8 as $I(q)q^4$ vs q and $I(q)q^2$ vs q. For the larger σ case (shown by O's), the oscillations are notably more distinct for the 400K PS as opposed to the 43K case. Also the scattering as $q \rightarrow 0$ is slightly larger for the 400K PS due to its

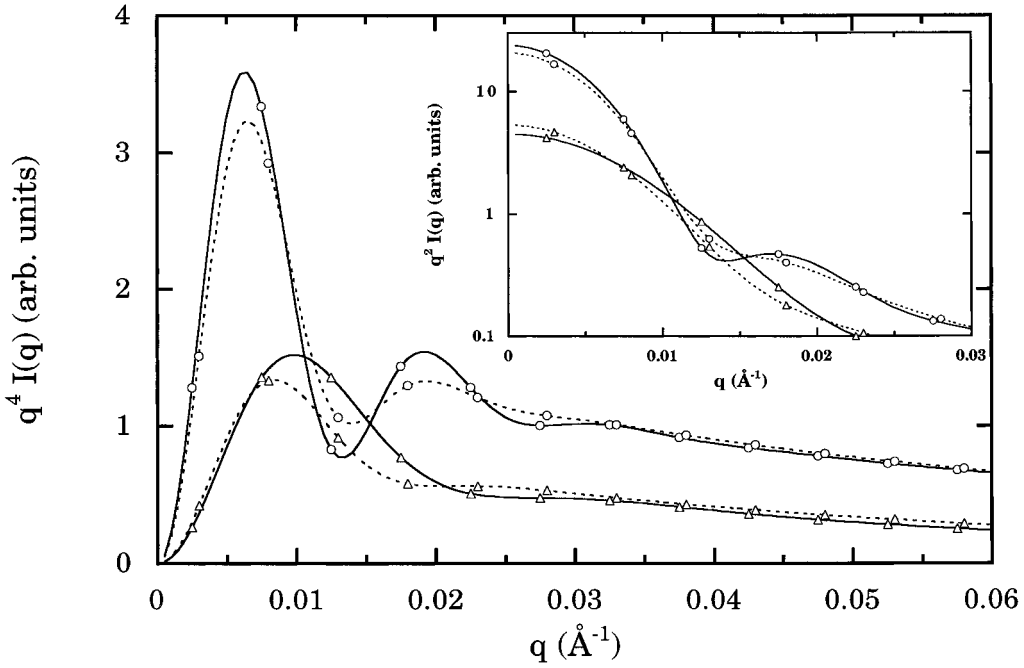

Figure 8. Small angle neutron scattering, plotted as $I(q)q^4$ vs q, resulting from large silica spheres or porous glass covered with a tethered polymer layer which has concentration profiles as in Figure 6. The same symbols are used as in Figure 6. An $I(q)q^2$ vs q plot is shown in the inset. A contrast match between the solvent and the glass and a radius of curvature much larger than the layer height have been assumed.

somewhat larger σ value. This is expected since the zero angle scattering $I(q\rightarrow 0)$ is proportional to the *square* of the grafting density. For the smaller σ, the tethered chain concentration profiles (with 400K and 43K PS mobile polymer) decay smoothly and the profile with 400K PS homopolymer does not appear to be steplike. As such the SANS shows only a single oscillation, and it is difficult to deconvolve the specific features of the concentrations profiles.

Comparing simulated NR (Figure 7) and SANS (Figure 8), it appears that the differences between the profiles in Figure 6 can be resolved nearly equally well (or equally poorly) using either NR or SANS. The issue of inverting NR or SANS data to obtain concentration profiles has been the subject of some discussion.[26] With regard to tethered polymer chains, Auroy and Auvray[24] determined concentration profiles using two independent contrast matching schemes. While this lends credence to their results, we point out that contrast variation can also be used in NR. In addition, there are other potential pitfalls in SANS which should be noted. In particular, it is difficult to accurately subtract incoherent scattering from the SANS data.[26] The analogous subtraction of diffuse scattering from reflectivity data is generally more straightforward.[22] Furthermore, for specimens grafted onto porous silica, the effects of curvature and roughness are assumed to be negligible when, in fact, the contribution from these sources is difficult to characterize. Indeed, it is easier to measure interfacial roughness with reflectivity. Nonetheless, in choosing between NR and SANS techniques to determine concentration profiles, it is advisable that the choice be made on the basis of the needs for a specific specimen geometry as well as the availability of a sensitive contrast scheme rather than a preference for a specific technique.

Conclusions

In summary, we have compared the results of SCF calculations and fits to NR data for tethered chains in contact with a solution of mobile polymer. While there is overall good qualitative agreement between the SCF results and fits to the NR data, the layer heights derived from the SCF data are systematically less than those fitted to the NR data. In addition, the calculated SCF profiles show subtle qualitative differences compared to the parabolic profiles used to fit the NR data; in particular, the SCF profiles become more steplike as both the surface density and the mobile homopolymer molecular weight increase. Computations to simulate the results of NR and SANS experiments suggest that it should be possible to discern the steplike nature of the profile for large homopolymer molecular weights only at high grafting density.

Acknowledgment. We would like to thank Lay-Theng Lee, Michael Kent, Sanat Kumar, and John van Zanten for critically reading the manuscript. C.M.W. acknowledges support from the Swedish Research Council for Engineering Science (TFR). B.J.F. gratefully acknowledges the support of the National Research Council Research Associateship Program during the course of this work.

References and Notes

(1) Halperin, A.; Tirrell, M.; Lodge, T. P. *Adv. Polym. Sci.* **1993**, *100*, 31.
(2) Milner, S. T. *Science* **1991**, *251*, 905.
(3) de Gennes, P.-G. *Macromolecules* **1980**, *13*, 1069.
(4) Gast, A. P.; Leibler, L. *Macromoecules* **1986**, *19*, 686.
(5) Zhulina, E. B.; Borisov, O. V.; Brombacher, L. *Macromolecules* **1991**, *24*, 4679.
(6) Wijmans, C. M.; Zhulina, E. B.; Fleer, G. *Macromolecules* **1994**, *27*, 3238.
(7) van Zanten, J. H. *Macromolecules* **1994**, *27*, 5052.
(8) Leibler, L. *Makrmol. Chem., Macromol. Symp.* **1988**, *16*, 1.
(9) Jones, R. A. L.; Norton, L. J.; Shull, K. R.; Kamer, E. J.; Felcher, G. P.; Karim, A.; Fetters, L. J. *Macromolecules* **1992**, *25*, 2359.
(10) Lee, L. T.; Factor, B. J.; Kent, M. S.; Rondelez, F. *J. Chem. Soc., Faraday Discuss.* **1994**, *98*, 139.
(11) Scheutjens, J. M. H. M.; Fleer, G. J. *J. Phys. Chem.* **1979**, *83*, 1619.
(12) Wijmans, C. M.; Scheutjens, J. M. H. M.; Zhulina, E. B. *Macromolecules* **1992**, *25*, 2657.
(13) Wijmans, C. M.; Leermakers, F. A. M.; Fleer, G. J. *J. Chem. Phys.* **1994**, *101*, 8214.
(14) Leermakers, F. A. M.; Scheutjens, J. M. H. M.; Gaylord, R. J. *Polymer* **1984**, *25*, 1577.
(15) Bandrup, J.; Immergut, E. J. *Polymer Handbook*, 3rd ed.; John Wiley & Sons: New York, 1989; p VII-178.
(16) Karim, A.; Tsukruk, V. V.; Douglas, J. F.; Satija, S. K.; Fetters, L. J.; Reneker, D. H.; Foster, M. D. *J. Phys. ii* **1995**, *5*, 1441.
(17) Kent, M. S.; Lee, L. T.; Factor, B. J.; Rondelez, F; Smith, G. S. *J. Chem. Phys.* **1995**, *103*, 2320. Kent, M. S.; Lee, L. T.; Factor, B. J.; Rondelez, F. *J. Phys. IV, Colloque C8*, **1993**, *3*, 49. Factor, B. J. ; Lee, L. T.; Kent, M. S.; Rondelez, F. *Phys. Rev. E* **1993**, *48*, 2354. Kent, M. S.; Lee, L. T.; Farnoux, B.; Rondelez, F. *Macromolecules* **1992**, *25*, 6240.
(18) Fleer, G. J.; Cohen Stuart, M. A.; Scheutjens, J. M. H. M.; Cosgrove, T.; Vincent, B. *Polymers at Interfaces*; Chapman & Hall: London, 1993, pp 472−474.
(19) Baranowski, R.; Whitmore, M. D. *J. Chem. Phys.* **1995**, *103*, 2343.
(20) Flory, P. J. *J. Chem. Phys.* **1949**, *17*, 303.
(21) Parrat, L. G. *Phys. Rev.* **1954**, *95*, 359.
(22) Russell, T. P. *Mater. Sci. Rep.* **1990**, *5*, 171.
(23) Auroy, P.; Auvray, L.; Leger, L. *Macromolecules* **1991**, *24*, 2523. Auroy, P.; Mir, Y.; Auvray, L. *Phys. Rev. Lett.* **1992**, *69*, 93.
(24) Auroy, P.; Auvray, L. *J. Phys. II France* **1993**, *3*, 227.
(25) Cosgrove, T.; Heath, T. G.; Ryan, K. *Langmuir* **1994**, *10*, 3500.
(26) Higgins, J. S.; Benoit, H. C. *Polymers and Neutron Scattering*, Oxford University Press: Oxford, U.K., 1994.

MA9514028